

Anatomy of Bridge Flutter: Some New Insights

Xinzhong Chen, Ahsan Kareem

*NatHaz Modeling Laboratory, University of Notre Dame, 156 Fitzpatrick Hall,
Notre Dame, IN, USA*

ABSTRACT: A new analysis framework that offers direct and explicit expressions for estimating the bimodal coupled flutter is presented. Its accuracy and effectiveness are demonstrated through a flutter analysis of a cable-stayed bridge. This framework is utilized to emphasize significance of the role played by both structural dynamics and aerodynamics on bridge flutter, which helps in better tailoring of the bridge structural systems and deck sections for superior bridge flutter performance. Based on this framework, guidance on the selection of modes and the role of different aerodynamic force components in multimode coupled flutter are offered. The potential importance of the consideration of inter-modal coupling in predicting bridge flutter dominated by the action of torsional mode is highlighted. Finally, a clear insight to the contribution of drag force to bridge flutter is provided.

KEYWORDS: Flutter, Wind loads, Aerodynamics, Aeroelasticity, Structural dynamics, Bridges.

1 INTRODUCTION

The flutter instability has primarily been the major concern in design of long span bridges that reiterates the needs for advanced understanding of wind-bridge interaction to meet the increasing safety and economic needs called for by increasing spans. The multimode flutter analysis framework has played an increasingly important role in seeking design solutions for advanced flutter performance of long span bridges (e.g., Scanlan 1978; Jones et al. 1998; Chen et al. 2000a). In this context, time domain analysis schemes facilitate consideration of nonlinearities in both structural dynamics and aerodynamics and the influence of turbulence on flutter (Diana et al. 1999; Chen et al. 2000b; Chen and Kareem 2003a).

The bimodal coupled flutter involving fundamental vertical bending and torsional modes has laid a firm foundation for understanding multimode coupled bridge flutter which is often dominated by the aerodynamic coupling of fundamental vertical bending and torsional modes with secondary contributions from other modes (Chen et al. 2000a). A step-by-step iterative analysis framework for bimodal coupled flutter presented in Matsumoto et al. (1997) has attempted to more closely capture the physics of bridge flutter.

The contributions of the motion-induced drag force and lateral motion-induced lift and pitching moment have been considered to be less important to bridge flutter. However, recent experience of the Akashi Kaikyo Bridge revealed the significant contribution of the torsional displacement induced drag force to the negative damping at the higher wind velocity range (Miyata et al. 1994). Since then, modeling and measurement of drag force and its potential importance to bridge flutter have been addressed (e.g., Jones et al. 1998), while a fundamental understanding of this issue remains unclear to the bridge aerodynamicists.

In this paper, a new framework that offers explicit expressions for estimating modal characteristics of bimodal coupled bridge system and for determining flutter condition is presented. Its accuracy and effectiveness are demonstrated through a flutter analysis of a cable-stayed bridge. This framework is utilized to emphasize the significance of role played by both

structural dynamics and aerodynamics on bridge flutter. Based on this framework, guidance on the selection of modes and the role of different aerodynamic force components in multimode coupled flutter are offered. The potential importance of consideration of inter-modal coupling in predicting bridge flutter dominated by the action of torsional mode is highlighted. Finally, a clear insight to the contribution of drag force to bridge flutter is provided.

2 THEORETICAL BACKGROUND

The bridge dynamic response components in the vertical, lateral and torsional directions, i.e., $h(x,t)$, $p(x,t)$ and $\alpha(x,t)$, respectively, around the statically deformed position, are expressed as

$$h(x,t) = \sum_j h_j(x)q_j(t); \quad p(x,t) = \sum_j p_j(x)q_j(t); \quad \alpha(x,t) = \sum_j \alpha_j(x)q_j(t) \quad (1)$$

where $h_j(x)$, $p_j(x)$ and $\alpha_j(x,t)$ are the j -th mode shapes in each respective direction; $q_j(t)$ is the j -th modal coordinate; and x is the spanwise position.

The self-excited forces per unit length linearized around the statically deformed position, i.e., lift (downward), drag (downwind) and pitching moment (nose-up), are given by (Scanlan 1978; Jones et al. 1998; Chen and Kareem 2002)

$$L_{se}(t) = \frac{1}{2} \rho U^2 (2b) \left(kH_1^* \frac{\dot{h}}{U} + kH_2^* \frac{b\dot{\alpha}}{U} + k^2 H_3^* \alpha + k^2 H_4^* \frac{h}{b} + kH_5^* \frac{\dot{p}}{U} + k^2 H_6^* \frac{p}{b} \right) \quad (2)$$

$$D_{se}(t) = \frac{1}{2} \rho U^2 (2b) \left(kP_1^* \frac{\dot{p}}{U} + kP_2^* \frac{b\dot{\alpha}}{U} + k^2 P_3^* \alpha + k^2 P_4^* \frac{p}{b} + kP_5^* \frac{\dot{h}}{U} + k^2 P_6^* \frac{h}{b} \right) \quad (3)$$

$$M_{se}(t) = \frac{1}{2} \rho U^2 (2b^2) \left(kA_1^* \frac{\dot{h}}{U} + kA_2^* \frac{b\dot{\alpha}}{U} + k^2 A_3^* \alpha + k^2 A_4^* \frac{h}{b} + kA_5^* \frac{\dot{p}}{U} + k^2 A_6^* \frac{p}{b} \right) \quad (4)$$

where ρ is the air density; U is the mean wind velocity; $B=2b$ is the bridge deck width; $k=\omega b/U$ is the reduced frequency; ω is the frequency of motion; and H_j^* , P_j^* and A_j^* ($j=1,2,\dots,6$) are the flutter derivatives that are functions of reduced frequency.

The governing equations of bridge motion in terms of the modal coordinates are given by

$$M\ddot{q} + C\dot{q} + Kq = \frac{1}{2} \rho U^2 (A_s q + \frac{b}{U} A_d \dot{q}) \quad (5)$$

where $M=\text{diag}[m_j]$, $C=\text{diag}[2m_j \zeta_j \omega_j]$ and $K=\text{diag}[m_j \omega_j^2]$ are the generalized mass, damping and stiffness matrices, respectively; m_j , ζ_j and ω_j are the j -th modal mass, damping ratio and frequency; A_s and A_d are the aerodynamic stiffness and damping matrices, respectively, and their elements are given by the following that represent terms involving the i and j -th modes:

$$A_{sij} = (2k^2) (H_4^* G_{h_i h_j} + H_6^* G_{h_i p_j} + bH_3^* G_{h_i \alpha_j} + P_6^* G_{p_i h_j} + P_4^* G_{p_i p_j} + bP_3^* G_{p_i \alpha_j} + bA_4^* G_{\alpha_i h_j} + bA_6^* G_{\alpha_i p_j} + b^2 A_3^* G_{\alpha_i \alpha_j}) \quad (6)$$

$$A_{dij} = (2k) (H_1^* G_{h_i h_j} + H_5^* G_{h_i p_j} + bH_2^* G_{h_i \alpha_j} + P_5^* G_{p_i h_j} + P_1^* G_{p_i p_j} + bP_2^* G_{p_i \alpha_j} + bA_1^* G_{\alpha_i h_j} + bA_5^* G_{\alpha_i p_j} + b^2 A_2^* G_{\alpha_i \alpha_j}) \quad (7)$$

and the modal integral $G_{r_i s_j} = \int_{span} r_i(x) s_j(x) dx$ (where $r, s=h, p, \alpha$).

The modal frequencies and damping ratios as well as inter-modal coupling of the bridge at a given wind velocity, with the contributions of aerodynamic stiffness and damping terms, can be analyzed through the solution of the following complex eigenvalue problem:

$$(\lambda^2 M + \lambda C + K)q_0 e^{\lambda t} = \frac{1}{2} \rho U^2 (A_s + \bar{\lambda} A_d) q_0 e^{\lambda t} \quad (8)$$

where $\lambda = -\xi\omega + i\omega\sqrt{1-\xi^2}$; ξ and ω are the damping ratio and frequency of the complex mode branch of interest; $\bar{\lambda} = \lambda b/U = (-\xi + i\sqrt{1-\xi^2})k$; and $i = \sqrt{-1}$. The flutter condition is determined by seeking the flutter onset velocity that corresponds to zero damping.

When the bridge is modeled by its fundamental vertical bending and torsional modes, i.e., $h_1(x) \neq 0$, $p_1(x)=0$, $\alpha_1(x)=0$ and $h_2(x)=0$, $p_2(x) \neq 0$, $\alpha_2(x) \neq 0$, and only the lift and pitching moment caused by the vertical and torsional motions are considered, the aerodynamic matrices are described by

$$A_s = (2k^2) \begin{bmatrix} H_4^* G_{h_1 h_1} & b H_3^* G_{h_1 a_2} \\ b A_4^* G_{h_1 a_2} & b^2 A_3^* G_{\alpha_2 a_2} \end{bmatrix}; \quad A_d = (2k) \begin{bmatrix} H_1^* G_{h_1 h_1} & b H_2^* G_{h_1 a_2} \\ b A_1^* G_{h_1 a_2} & b^2 A_2^* G_{\alpha_2 a_2} \end{bmatrix} \quad (9)$$

By assuming that $A_s + \bar{\lambda} A_d \approx A_s + ik A_d$, $2\xi^2 \omega^2 \approx 0$, $2\bar{\xi}_1 \bar{\xi} \bar{\omega}_1 \omega \approx 0$, $2\bar{\xi}_2 \bar{\xi} \bar{\omega}_2 \omega \approx 0$ and $\sqrt{1-\xi^2} \approx 1$, Eq. (8) can be rewritten as

$$m_1 [-\omega^2 + i2(\bar{\xi}_1 \bar{\omega}_1 - \xi\omega)\omega + \bar{\omega}_1^2] q_{10} e^{\lambda t} = \frac{1}{2} \rho U^2 (A_{s12} + ik A_{d12}) q_{20} e^{\lambda t} \quad (10)$$

$$m_2 [-\omega^2 + i2(\bar{\xi}_2 \bar{\omega}_2 - \xi\omega)\omega + \bar{\omega}_2^2] q_{20} e^{\lambda t} = \frac{1}{2} \rho U^2 (A_{s21} + ik A_{d21}) q_{10} e^{\lambda t} \quad (11)$$

where $\bar{\omega}_j$ and $\bar{\xi}_j$ ($j=1, 2$) are the frequencies and damping ratios that include contributions from uncoupled aerodynamic stiffness and damping terms:

$$\bar{\omega}_1 = \omega_1 \left[1 - \frac{\rho b^2 H_4^* G_{h_1 h_1}}{m_1} \left(\frac{\omega}{\omega_1} \right)^2 \right]^{1/2}; \quad \bar{\xi}_1 = \frac{\xi_1 \omega_1}{\bar{\omega}_1} - \frac{\rho b^2 H_1^* G_{h_1 h_1}}{2m_1} \left(\frac{\omega}{\bar{\omega}_1} \right) \quad (12)$$

$$\bar{\omega}_2 = \omega_2 \left[1 - \frac{\rho b^4 A_3^* G_{\alpha_2 a_2}}{m_2} \left(\frac{\omega}{\omega_2} \right)^2 \right]^{1/2}; \quad \bar{\xi}_2 = \frac{\xi_2 \omega_2}{\bar{\omega}_2} - \frac{\rho b^4 A_2^* G_{\alpha_2 a_2}}{2m_2} \left(\frac{\omega}{\bar{\omega}_2} \right) \quad (13)$$

Consider the solution of the mode branch with the frequency ω that is closer to $\bar{\omega}_1$ than $\bar{\omega}_2$. The complex mode shape in terms of bq_{20}/q_{10} can be determined from Eq. (11) as

$$\frac{bq_{20}}{q_{10}} = \Phi e^{i\phi} = \left(\frac{\rho b^4}{m_2} \right) \frac{(A_4^* + iA_1^*) G_{h_1 a_2}}{[-1 + (\bar{\omega}_2/\omega)^2 + i2\bar{\xi}_2' \bar{\omega}_2/\omega]} \quad (14)$$

where $\bar{\xi}_2' = \bar{\xi}_2 - \xi\omega/\bar{\omega}_2$. Accordingly, the amplitude ratio and phase difference are given by

$$\Phi = \left(\frac{\rho b^4}{m_2} \right) \frac{\sqrt{(A_4^*)^2 + (A_1^*)^2} G_{h_1 a_2}}{\sqrt{[1 - (\bar{\omega}_2/\omega)^2]^2 + (2\bar{\xi}_2' \bar{\omega}_2/\omega)^2}}; \quad \phi = \tan^{-1} \left(\frac{A_1^*}{A_4^*} \right) + \tan^{-1} \left(\frac{2\bar{\xi}_2' \bar{\omega}_2/\omega}{1 - (\bar{\omega}_2/\omega)^2} \right) - \pi \quad (15)$$

The frequency and damping ratio of the mode branch are then determined from Eq. (10) as

$$\omega = \omega_1 \left[1 + \left(\frac{\rho b^2}{m_1} \right) H_4^* G_{h_1 h_1} + \Phi' \cos \phi' \right]^{-1/2}; \quad \xi = \frac{\xi_1 \omega_1}{\omega} - \left(\frac{\rho b^2}{2m_1} \right) H_1^* G_{h_1 h_1} - \frac{1}{2} \Phi' \sin \phi' \quad (16)$$

$$\Phi' = \left(\frac{\rho b^2}{m_1} \right) \left(\frac{\rho b^4}{m_2} \right) \frac{\sqrt{(H_3^*)^2 + (H_2^*)^2} \sqrt{(A_4^*)^2 + (A_1^*)^2} G_{h_1 \alpha_2}^2}{\sqrt{[1 - (\bar{\omega}_2 / \omega)^2]^2 + (2\bar{\xi}_2' \bar{\omega}_2 / \omega)^2}} \quad (17)$$

$$\phi' = \tan^{-1} \left(\frac{H_2^*}{H_3^*} \right) + \tan^{-1} \left(\frac{A_1^*}{A_4^*} \right) + \tan^{-1} \left(\frac{2\bar{\xi}_2' \bar{\omega}_2 / \omega}{1 - (\bar{\omega}_2 / \omega)^2} \right) - \pi \quad (18)$$

Similar expressions can be derived for the mode branch with the frequency ω that is closer to $\bar{\omega}_2$ than $\bar{\omega}_1$. The complex mode shape in terms of $q_{10}/(bq_{20})$ is given by

$$\frac{q_{10}}{bq_{20}} = \Psi e^{i\psi} = \left(\frac{\rho b^2}{m_1} \right) \frac{(H_3^* + iH_2^*) G_{h_1 \alpha_2}}{[-1 + (\bar{\omega}_1 / \omega)^2 + i2\bar{\xi}_1' \bar{\omega}_1 / \omega]} \quad (19)$$

where $\bar{\xi}_1' = \bar{\xi}_1 - \xi \omega / \bar{\omega}_1$. Accordingly, the amplitude ratio and phase difference are given by

$$\Psi = \left(\frac{\rho b^2}{m_1} \right) \frac{\sqrt{(H_3^*)^2 + (H_2^*)^2} G_{h_1 \alpha_2}}{\sqrt{[1 - (\bar{\omega}_1 / \omega)^2]^2 + (2\bar{\xi}_1' \bar{\omega}_1 / \omega)^2}}; \quad \psi = \tan^{-1} \left(\frac{H_2^*}{H_3^*} \right) + \tan^{-1} \left(\frac{2\bar{\xi}_1' \bar{\omega}_1 / \omega}{1 - (\bar{\omega}_1 / \omega)^2} \right) - \pi \quad (20)$$

and the frequency and damping ratio of the mode branch are given by

$$\omega = \omega_2 \left[1 + \left(\frac{\rho b^4}{m_2} \right) A_3^* G_{\alpha_2 \alpha_2} + \Psi' \cos \psi' \right]^{-1/2}; \quad \xi = \frac{\bar{\xi}_2' \omega_2}{\omega} - \left(\frac{\rho b^4}{2m_2} \right) A_2^* G_{\alpha_2 \alpha_2} - \frac{1}{2} \Psi' \sin \psi' \quad (21)$$

$$\Psi' = \left(\frac{\rho b^2}{m_1} \right) \left(\frac{\rho b^4}{m_2} \right) \frac{\sqrt{(H_3^*)^2 + (H_2^*)^2} \sqrt{(A_4^*)^2 + (A_1^*)^2} G_{h_1 \alpha_2}^2}{\sqrt{[1 - (\bar{\omega}_1 / \omega)^2]^2 + (2\bar{\xi}_1' \bar{\omega}_1 / \omega)^2}} \quad (22)$$

$$\psi' = \tan^{-1} \left(\frac{H_2^*}{H_3^*} \right) + \tan^{-1} \left(\frac{A_1^*}{A_4^*} \right) + \tan^{-1} \left(\frac{2\bar{\xi}_1' \bar{\omega}_1 / \omega}{1 - (\bar{\omega}_1 / \omega)^2} \right) - \pi \quad (23)$$

It should be noted that all flutter derivatives in the preceding expressions are defined at the respective reduced frequency of each mode branch. Each modal frequency is often very close to the respective frequency that only includes the contribution from uncoupled aerodynamic terms, i.e., $\bar{\omega}_1$ or $\bar{\omega}_2$. In addition, the influences of damping ratio ξ on the amplitude ratio and phase difference are often small and even can be neglected by setting $\xi=0$, particularly, in cases where $\bar{\omega}_1$ and $\bar{\omega}_2$ are well separated and ξ is relatively low. Therefore, while iterative calculations for both frequency and damping ratio of each mode branch are required, they converge very fast. The iterative calculations may even be eliminated by using their values at a slightly lower wind velocity, or even by using the values at zero wind velocity.

It is very important to emphasize that the proposed framework invoked approximations related only to the damping ratio. In fact, a similar approximation has implicitly been made in the definition of flutter derivatives which have traditionally been assumed to be independent of damping. Different treatments of damping in the aerodynamic modeling can also be observed in flutter analysis schemes such as so-called p - k and p methods (e.g., Chen et al. 2000a). At the flutter onset velocity with zero damping, the proposed framework for the flutter mode branch results in the exact solution as the invoked approximations vanish.

3 ILLUSTRATION AND DISCUSSION

In the following, the accuracy and effectiveness of the proposed framework is demonstrated using a long span cable-stayed bridge with a center span of about 1000 m. The modal damping

ratio for the fundamental vertical bending and torsional modes, i.e., modes 3 and 13, are assumed to be 0.0032. Only the lift and pitching moment acting on the bridge deck related to flutter derivatives H_i^* , A_i^* ($i=1, 2, 3, 4$) are considered. For comparison, two cases referred to as cases A and B respectively corresponding to a slender and a bluff bridge deck section are considered. In case A, the flutter derivatives are calculated from Theoderson function, H_1^* , H_3^* , H_4^* , $A_2^* < 0$, and H_2^* , A_1^* , A_3^* , $A_4^* > 0$. In case B, they are measured using a rectangular section with width to height ratio of 5 (Matsumoto et al. 1997), H_1^* , H_3^* , H_4^* , $A_4^* < 0$, $H_2^* > 0$, $A_1^* > 0$ then < 0 , $A_2^* < 0$ then > 0 , and $A_3^* > 0$ then < 0 as the reduced wind velocity increases.

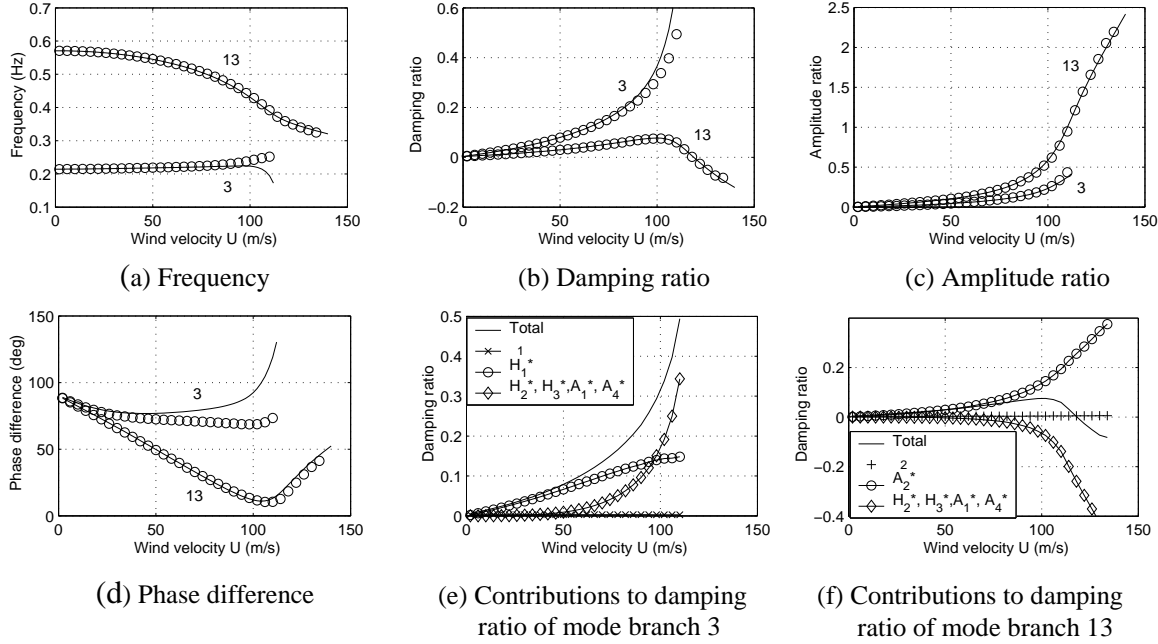


Fig. 1 Comparison of flutter analysis for the cable-stayed bridge in case A

Figs. 1(a) to 1(d) show the predicted frequencies and damping ratios as well as mode shapes in terms of amplitude ratios and phase differences for both mode branches in case A. The amplitude ratios are given in terms of the ratio between the vertical and torsional displacements of the bridge deck at the main span center so that these are independent of the normalization scheme of the mode shapes. The solid lines and circles respectively correspond to the complex eigenvalue analysis and the analysis based on the proposed framework. Fig. 2 shows the results for case B. It can be seen that the proposed framework provides predictions for both branches that show a good agreement with the complex eigenvalue analysis. There are some minor differences between the two approaches, which only surface at high values of damping. This demonstrates the accuracy and effectiveness of the proposed framework.

The proposed framework clearly highlights the contributions of different aerodynamic force components to damping ratios of two mode branches (Eqs. (16) and (21)). Figs. 1(e) and 1(f) show the result in case A where the term A_2^* , for example, represents $-\rho b^4 / (2m_2) A_2^* G_{\alpha_2 \alpha_2}$. As $A_2^* < 0$, no torsional flutter exists at the action of only the single torsional mode. However, the coupled aerodynamic forces generate negative damping which leads the bridge to a coupled flutter initiated from the torsional mode branch at 119 m/s. In contrast, for the vertical mode branch, the coupled forces result in an increase in damping. This opposite contribution of the coupled forces are attributed to the different signs of $\sin\phi'$ and $\sin\psi'$, which are mainly attributed to the different values of $\bar{\omega}_2/\omega$ and $\bar{\omega}_1/\omega$ for these two mode branches. This contrasting behavior clearly points at the energy transfer between these two mode branches.

Figs. 2(e) and 2(f) show the results in case B. As A_2^* turns to positive from negative with wind velocity increases, a torsional flutter exists beyond 69.6 m/s even at the action of single torsional mode. While the contribution of the coupled forces is relatively weak, it reduces the damping of the torsional mode branch and leads to a lower flutter onset velocity of 64.3 m/s. This suggests that the multimode coupled flutter analysis framework is generally required for not only bridges with slender sections but also bridges with relatively bluff sections as has been pointed out in Chen et al. (2000a). Consideration of inter-modal coupling is potentially more important in the cases of a soft-type flutter in which negative damping builds up slowly with increasing wind velocity.

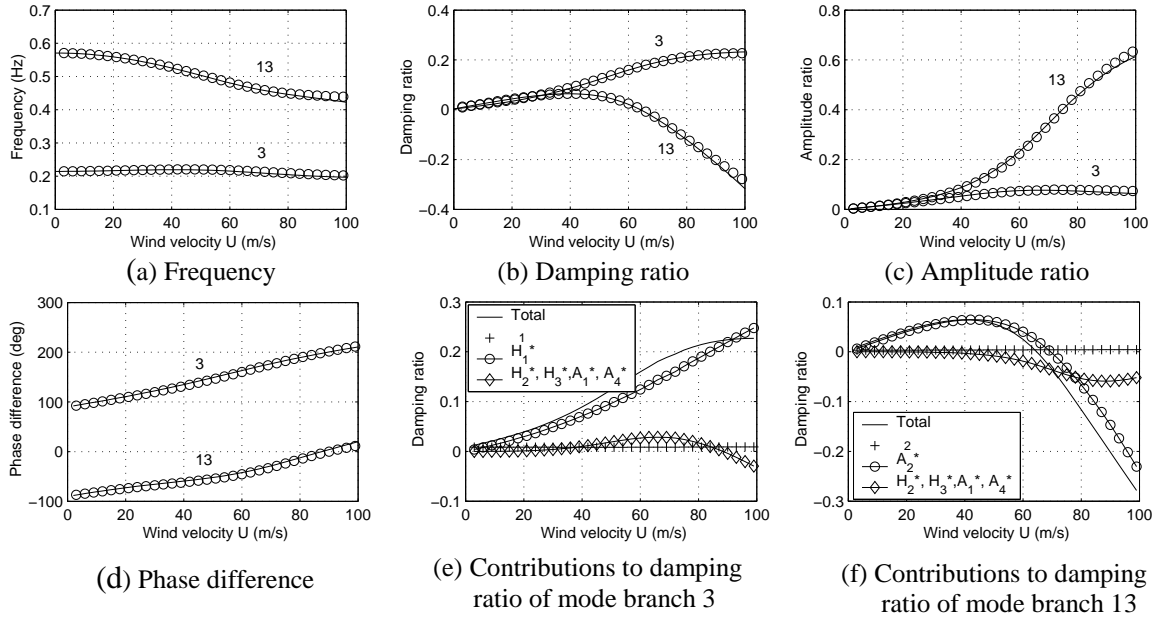


Fig. 2 Comparison of flutter analysis for the cable-stayed bridge in case B

The proposed framework offers valuable insights to the significance of the both structural dynamics and aerodynamics on coupled bridge flutter that help in developing design solutions to enhance flutter performance. For instance, increases in structural mass and torsional frequency as well as the frequency ratio between the torsional and vertical modes help to improve flutter performance. Higher structural damping contributes not only to the increase in the damping of the respective mode branch but also to the reduction of coupled motion and therefore is beneficial to flutter. Modification of bridge structural system can potentially change structural dynamics including mode shapes hence the modal integrals and the contributions of aerodynamic forces. The uncoupled self-excited forces due to displacements, i.e., terms related to H_4^* and A_3^* , in particular, A_3^* , reduce the modal frequencies thus have unfavorable influences on flutter. The uncoupled self-excited forces due to bridge velocities, i.e., terms related to H_1^* and A_2^* , in particular, A_2^* , increase the modal damping thus is beneficial to flutter. The negative damping generated by the coupled forces, i.e., terms related to H_2^* , H_3^* , A_1^* and A_4^* , particularly, H_3^* and A_1^* , is the main source that drives bridge to coupled flutter instability. In order to improve and better tailor bridge flutter performance, it is essential to enhance the beneficial and reduce the unfavorable contributions to system damping. It can be realized through the introduction of aerodynamically tailored bridge decks and effective bridge structural systems.

The proposed framework also helps to understand the participation of structural modes in a multimode coupled flutter, which can guide the selection of modes in a flutter analysis. It is clear that a mode comprising of large values of coupled terms in aerodynamic stiffness and damping with the torsional mode of interest, which are functions of flutter derivatives and modal integrals,

is more likely to be coupled with the torsional mode. This coupling will be enhanced when its damping is low and its frequency is close to the torsional frequency. The modes that are most likely to be excited should be considered in the analysis. The understanding of modes that play a major role in flutter not only helps in better understand multimode coupled bridge flutter, but equally offers valuable information on the design and interpretation of wind tunnel studies using full aeroelastic bridge models which may only replicate a limited number of modes of the prototypes.

4 INTER-MODAL COUPLING AND CONTRIBUTION OF DRAG FORCE

Fig. 3 shows the predicted frequencies and damping ratios of mode branches 3, 10 and 13, for the cable-stayed bridge with the bluff deck section (case B). Mode 10 is the second symmetric lateral bending mode with coupled motion in torsion. The results for cases that include and ignore the inter-modal coupling are compared. Without the consideration of inter-modal coupling, the action of mode 13 leads to a torsional flutter beyond 69.6 m/s and the action of mode 10 develops a torsional flutter beyond 74.3 m/s. The aerodynamic damping of mode 10 is very low as compared to mode 13. With the consideration of inter-modal coupling, the curve veering of frequency and damping loci of mode branches 10 and 13 is observed at about 80 m/s where these two modal frequencies are close to each other. The curve veering is due to strong interactions of these two modes (Chen and Kareem 2003). These two mode branches continuously exchange their properties as these experience veering. At the end of veering action, mode branch 13 becomes dominated by structural mode 10, and mode branch 10 is dominated by structural mode 13. Based on the expression for the amplitude ratio, it is clear that the coupling between modes 10 and 13 becomes significant only at the region where their frequencies are close to each other. A negative peak in the damping loci of mode branch 13 at the wind velocity of around 80 m/s clearly indicates this strong interaction. The flutter onset velocities for these two branches are 58.7 m/s and 65.9 m/s. Results demonstrate the importance of inter-modal coupling for flutter prediction of bridges with even bluff deck sections.

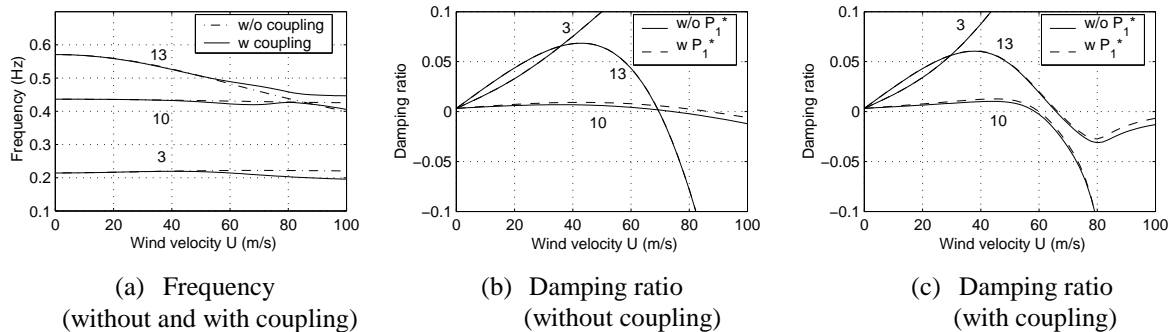


Fig. 3 Influence of inter-modal coupling and drag force on torsional flutter

In Figs. 3(b) and 3(c), the influence of drag damping force related to $P_1^* = -2C_D/k$ (where $C_D=0.2$ is the static drag force coefficient) is presented. It is seen that, while the additional damping associated with the lateral motion is small, it apparently increases the flutter onset velocity of the torsional flutter initiated from mode 10 from 74.3 m/s to 86.8 m/s. However it has almost no influence on the torsional flutter initiated from mode 13. The influence of drag force on these mode branches become negligible when the inter-modal coupling is further considered as shown in Fig. 3(c).

This relative significance of different force components or flutter derivatives can be easily clarified based on the Eqs. (6) and (7) and the framework presented in this study. The drag force may become relatively important such as in the case of soft-type flutter as demonstrated in Fig.

3(b) for mode 10. However, the contribution of drag force will remain insignificant in the cases of hard-type flutter where aerodynamic damping generated by lift and pitching moment rapidly develops as wind velocity increases as demonstrated in Fig. 3(b) for mode 13 and in Fig. 3(c) for both mode branches 10 and 13. It is noteworthy that the flutter analysis framework that offers information concerning changes in modal frequencies and damping ratios and associated mode shapes with increasing wind velocity provides more valuable insights to the physics of multimode coupled flutter in comparison with the analysis that only focuses on the evaluation of flutter onset velocity.

5 CONCLUDING REMARKS

A new analysis framework with direct and explicit expressions for estimating bimodal coupled flutter was presented and its accuracy and effectiveness were demonstrated by way of examples. This framework offered valuable insights to the significance of both structural dynamics and aerodynamics to bridge flutter that helped in enhancing bridge flutter performance. This framework helped in providing improved understanding of the inter-modal coupling and the role of each mode to coupled bridge flutter. The example of cabled-stayed bridge with relatively bluff deck section highlighted the potential importance of inter-modal coupling in torsional flutter. The discussion concerning the influence of drag force and curve veering of eigenvalue loci aided further in enhancing our understanding of the physics of bridge flutter.

6 ACKNOWLEDGMENT

The authors are grateful for the financial support provided in part by the National Science Foundation grant CMS 00-85109.

7 REFERENCES

- Chen, X. and Kareem, A. (2002). "Advances in the modeling of aerodynamic forces on bridge decks." *J. of Eng. Mech.*, ASCE, 128(11), 1193-1205.
- Chen, X. and Kareem, A. (2003a). "Aeroelastic analysis of bridges: effects of turbulence and aerodynamic nonlinearities." *J. of Eng. Mech.*, ASCE, 129(8) (in press).
- Chen, X. and Kareem, A. (2003b). "Curve veering of eigenvalue loci of bridges with aeroelastic effects." *J. of Eng. Mech.*, ASCE, 129(2), 146-159.
- Chen, X., Matsumoto, M. and Kareem, A. (2000a). "Aerodynamic coupling effects on flutter and buffeting of bridges." *J. of Eng. Mech.*, ASCE, 126(1), 17-26.
- Chen, X., Matsumoto, M. and Kareem, A. (2000b). "Time domain flutter and buffeting response analysis of bridges." *J. of Eng. Mech.*, ASCE, 126(1), 7-16.
- Diana, G., Cheli, F., Zasso, A. and Boccione, M. (1999). "Suspension bridge response to turbulent wind: Comparison of new numerical simulation method results with full scale data." *Wind Eng. into the 21 Century*, A. Larsen, G. L. Larose and F. M. Livesey (eds), Balkema, Rotterdam, The Netherlands, 871-878.
- Jones, N. P., Scanlan, R. H., Jain A. and Katsuchi, H. (1998). "Advances (and challenges) in the prediction of long-span bridge response to wind." *Bridge Aerodyn.*, A. Larsen and S. Esdahl (eds), Balkema, Rotterdam, The Netherlands, 59-85.
- Miyata, T., Tada, K., Sato, H., Katsuchi, H. and Hikami, Y. (1994). "New findings of coupled flutter in full model wind tunnel tests on the Akashi Kaikyo Bridge." *Proc. of Symp. on Cable-Stayed and Suspension Bridges*, Deauville, France, October 12-15, 163-170.
- Matsumoto, M., Daito, Y., Yoshizumi, F., Ichikawa, Y. and Yabutani, T. (1997). "Torsional flutter of bluff bodies." *J. of Wind Eng. Ind. Aerodyn.*, 69-71, 871-882.
- Scanlan, R. H. (1978). "The action of flexible bridges under wind, 1: flutter theory." *J. of Sound and Vib.*, 60(2), 187-199.